

Small molecules control the formation of Pt nanocrystals: a key role of carbon monoxide in the synthesis of Pt nanocubes†

Binghui Wu, Nanfeng Zheng* and Gang Fu*

Received 5th September 2010, Accepted 21st October 2010

DOI: 10.1039/c0cc03671d

In many previous studies, nonaqueous synthesis of Pt nanocubes with tunable size has been achieved by the use of metal carbonyls (e.g., $\text{Fe}(\text{CO})_5$, $\text{Co}_2(\text{CO})_8$, $\text{W}(\text{CO})_6$). The presence of zero-valent metals in the carbonyls was demonstrated as the key factor to the nanocube formation but the role of CO was entirely ignored. By using CO alone, we have now demonstrated that the favorable growth of Pt nanocubes in the presence of CO is mainly owing to the effect that the Pt (100) surface is stabilized by the co-adsorption of CO and amine.

Colloidal nanoparticles of platinum have been extensively explored for catalytic applications in automobile exhaust purification, petrochemical industry, fuel-cell technology, and fine chemical industry.¹ As a surface-dependent property, the catalysis by metal nanocrystals is often determined by their surface structure.^{2–7} For instance, {100} terminated Pt nanocubes have been reported to exhibit significantly enhanced electrocatalytic activity in oxygen reduction reaction.^{7,8} Therefore, the development of effective synthetic methods aimed to tailor the size and shape of Pt nanocrystals is important for their catalysis applications.^{3,6,7} However, as compared to Au or Ag, the surface energy difference among various crystallographic planes of Pt is relatively large, resulting in a challenge in controlling the shape of Pt nanoparticles.²

Recently, there have been an increasing number of reports on the synthesis of Pt nanocrystals with high-energy facets using electrochemistry,^{9–12} aqueous,^{6,13–15} and nonaqueous synthetic routes.^{7,16–20} Several effective nonaqueous synthetic methods have been developed to prepare monodispersed Pt nanocubes. The nonaqueous syntheses of Pt nanocubes were mainly achieved by reducing Pt precursors in an H_2 atmosphere^{16,17} or in the presence of metal carbonyls, such as $\text{Fe}(\text{CO})_5$,^{7,18} $\text{Co}_2(\text{CO})_8$,¹⁹ and $\text{W}(\text{CO})_6$.²⁰ The distinct advantage of the carbonyl route over the hydrogen reduction method is that monodispersed well-defined Pt nanocubes can be synthesized in comparatively high concentrations. In all previous studies of the carbonyl routes, the zero-valent metals (i.e., Fe, Co, W) in the metal carbonyls were considered to play an essential role for the shape control of Pt nanocubes. The possible role of CO decomposed from the carbonyls was entirely ignored. Considering that the strong binding of CO

to Pt,²¹ we however believe that CO should play an important role in the formation of Pt nanocubes where metal carbonyls were used.

In order to demonstrate that CO alone was able to determine the formation of Pt nanocubes, we excluded the use of any metal carbonyl in our studies. The nonaqueous syntheses of Pt nanoparticles were carried out by reducing $\text{Pt}(\text{acac})_2$ in mixtures containing oleylamine (OAm) and oleic acid (OLA) in various ratios (see ESI† for details). We first chose 4 : 1 (volume ratio) OAm/OLA mixture as the solvent for the studies. In the absence of any metal carbonyl or CO, as illustrated in Fig. 1a, the thermal decomposition of $\text{Pt}(\text{acac})_2$ at 180 °C in the 4 : 1 OAm/OLA mixed solvent led to the formation of Pt nanodendrites, consistent with previous studies.^{19,20} Surprisingly, when a CO gas flow ($\sim 30 \text{ mL min}^{-1}$) was simply applied on the surface of the same reaction, the formation of Pt nanocrystals in cubic shape was observed (Fig. 1b, Fig. S1, ESI†). The average edge length of the as-prepared Pt nanocubes was 10.3 nm. As revealed by high-resolution TEM (HRTEM), the well-resolved lattice fringes indicate the single-crystallinity of the Pt nanocubes (Fig. 1c). The lattice fringes running parallel to the edges of the cube

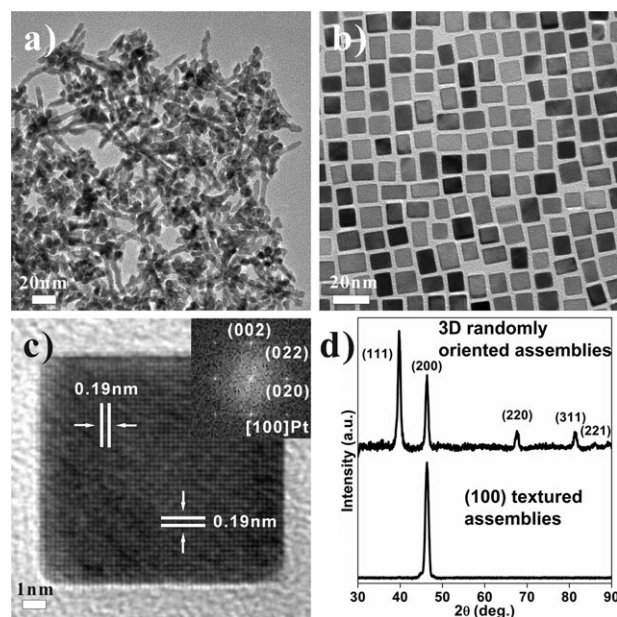


Fig. 1 TEM images of (a) Pt nanodendrites synthesized without CO and (b) 10.3 nm Pt nanocubes prepared under CO flow at 180 °C, both using 4 : 1 OAm/OLA solvent. (c) HRTEM and fast Fourier transform (inset) of an individual 10.3 nm Pt nanocube shown in (b). (d) XRD patterns of randomly oriented and (100) textured Pt nanocube assemblies.

State Key Laboratory for Physical Chemistry of Solid Surfaces and Department of Chemistry, College of Chemistry and Chemical Engineering, Xiamen University, Xiamen 361005, China.

E-mail: nfzheng@xmu.edu.cn, gfu@xmu.edu.cn;
Fax: +86 592 2183047; Tel: +86 592 2186821

† Electronic supplementary information (ESI) available: TEM images of Pt nanoparticles made in mixed OAm and OLA, FT-IR, XRD, CV of 10.3 nm Pt nanoparticles, and computational details. See DOI: 10.1039/c0cc03671d

have a spacing of 0.19 nm which corresponds to the (200) interplanar distance of face centered cubic (fcc) platinum.

The highly crystalline nature of the as-prepared Pt nanocubes was also confirmed by X-ray diffraction (XRD) analysis. As shown in Fig. 1d, when the analysis was run on the random aggregates of the Pt nanocubes deposited on a rough glass holder, all characteristic diffraction peaks of fcc Pt were observed. In comparison, slow evaporation of the Pt nanocube dispersion on a surface-polished Si(100) wafer resulted in an oriented assembly of the Pt nanocubes. In the resultant XRD pattern, the (200) peak intensity was significantly enhanced while the (111) disappeared. This observation indicates that the Pt nanocubes in the oriented assembly align perfectly flat on the substrates with their {100} facets, further confirming that the as-prepared Pt nanocubes have a very narrow distribution of shape. The average crystalline size estimated from Scherrer's formula using the (200) peak was ~ 10.2 nm, consistent with the average edge length that was measured in the TEM images.

While no Pt nanocubes were produced in the absence of CO, high-quality Pt nanocubes were readily prepared by introducing surface CO gas flow. This result suggested the importance of CO in the formation of Pt nanocubes, which could originate from the strong binding of CO on Pt. We have therefore used FT-IR to check the presence of CO adsorption on the as-made 10.3 nm Pt nanocubes. While no CO adsorption was observed on Pt nanodendrites prepared in absence of CO (Fig. S2, ESI[†]), the freshly prepared Pt nanocubes displayed an obvious CO band at 2082 cm^{-1} and a weak band at 1802 cm^{-1} (Fig. 2), attributed to linear and bridging CO respectively. The CO signal slowly decayed over time but was still strongly present in the Pt nanocubes after 120 h exposure in air (Fig. S3, ESI[†]). The IR studies (Fig. S2, ESI[†]) also revealed that only OAm was present in the as-prepared Pt nanocubes although both OAm and OLA were used, consistent with the previous report.²⁰ In order to explain the origin of shape control using CO, we calculated the surface energies (ϕ) of the (100) and (111) facets of Pt before and after adsorption of amine (RNH₂) and/or CO (see ESI[†] for details). The periodic DFT calculations (Table S1, ESI[†]) revealed that for clean Pt surface, ϕ_{100} is higher than ϕ_{111} by 0.26 eV per atom. When RNH₂ adsorbs on the surfaces at 0.25 monolayer (ML), the difference ($\Delta\phi$) between ϕ_{100} and ϕ_{111} decreases to

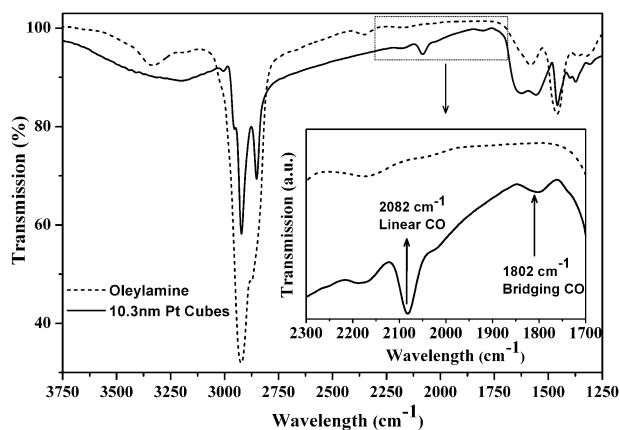


Fig. 2 IR spectra of as-received oleylamine and the 10.3 nm Pt nanocubes prepared in 4 : 1 OAm/OLA mixed solvent.

0.20 eV per atom. After co-adsorption of RNH₂ and CO (0.25 ML/0.25 ML), $\Delta\phi_{(100)-(111)}$ is calculated to be -0.02 eV per atom, indicating that (100) facet becomes more stable than (111) facet. Thus, experiments and theoretical calculations reach an agreement that CO adsorption plays a crucial role in the formation of Pt nanocubes, which is different from the mechanism proposed in the syntheses of Pt or Pt₃M nanocubes where metal carbonyls were used. In those systems, the presence of zero-valent metals (*i.e.*, Fe, Co, W) in the carbonyls has been regarded as the key to the nanocube formation. It is worth noting that CO binding was also observed on the Pt nanocubes synthesized by using W(CO)₆ (Fig. S4, ESI[†]).²⁰

Besides the use of metal carbonyl, the OAm/OLA ratio was also claimed as an important factor to the formation of Pt nanocubes in many previous studies.²⁰ However, based on our proposal that the co-adsorption of CO and amine on Pt(100) is the most essential reason for the nanocube formation, one would expect that Pt nanocubes could be prepared even in pure OAm. However, when the reaction was carried out in pure OAm in the presence of surface CO gas flow, only well-dispersed Pt polyhedral nanocrystals were produced (Fig. 3a). Detailed analysis revealed that the major Pt polyhedra were cuboctahedra with an average size of 5.0 nm, which did not seem to follow the prediction from our hypothesis on the role of CO. As indicated by the fact that only OAm was present in the Pt nanocubes prepared in 4 : 1 OAm/OLA mixture, OAm bound strongly on the surface of Pt nanoparticles. Considering that CO gas flowed only on the surface of the reactions, the interaction of OAm on Pt could be strong enough to compete with the CO binding. To obtain nanocubes in pure OAm, the CO adsorption on Pt must be enhanced. Following this line, we have succeeded in obtaining Pt nanocubes in pure OAm by applying higher CO pressure.

Under 1 atm CO instead of surface CO gas flow, Pt nanocubes were indeed produced from the reactions, although some truncated nanocubes were also observed (Fig. 3b). The average edge length of the as-prepared nanocubes was 5.1 nm. When the CO pressure was further increased to 2 atm, the cubic morphology of the prepared nanoparticles was maintained. However, their average edge length was reduced to 4.1 nm (Fig. 3c). It should be pointed out that the thermal reduction of Pt(acac)₂ in pure OAm at 180 °C hardly took place, suggesting the additional role of CO as the reductant in the synthesis. The faster nucleation caused by the higher CO pressure could explain the size reduction of Pt nanocubes under increased CO pressure. Both HRTEM and XRD analysis (Fig. 3, Fig. S5, ESI[†]) suggested that Pt

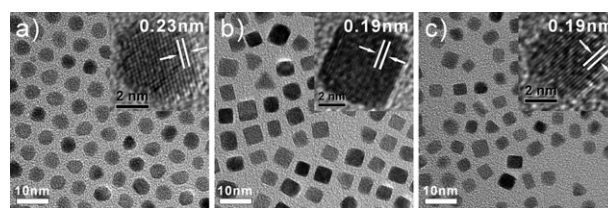


Fig. 3 Representative TEM images of Pt nanoparticles in pure OAm under (a) CO flow, (b) 1 atm and (c) 2 atm CO. The insets are the corresponding HRTEM images.

nanocubes prepared under higher CO pressures were of high quality. Furthermore, our preliminary results demonstrated that the surface of the as-prepared Pt nanocubes was readily activated by exchanging with *n*-butylamine to provide a clean surface for electrocatalysis studies (Fig. S6, ESI†).²²

In conclusion, we have developed an effective method to control the formation of Pt nanocubes by introducing CO. While FT-IR measurements confirmed the co-adsorption of CO and oleylamine on the as-prepared Pt nanocubes, periodic DFT calculations revealed that Pt (100) surface can be significantly stabilized by the co-adsorption of CO and oleylamine. By understanding the key role of CO adsorption, the synthesis of Pt nanocubes has now been successfully achieved in the mixtures of OAm and OLA, and also in pure OAm.

We thank NSFC (20925103, 20871100, 20721001), the Fok Ying Tung Education Foundation (121011), MSTC (2011CB932403, 2009CB930703), NSF of Fujian Province for Distinguished Young Investigator Grant (2009J06005) and the Key Scientific Project of Fujian Province (2009HZ0002-1).

Notes and references

- 1 A. C. Chen and P. Holt-Hindle, *Chem. Rev.*, 2010, **110**, 3767–3804.
- 2 Z. Y. Zhou, N. Tian, Z. Z. Huang, D. J. Chen and S. G. Sun, *Faraday Discuss.*, 2008, **140**, 81–92.
- 3 C. K. Tsung, J. N. Kuhn, W. Y. Huang, C. Aliaga, L. I. Hung, G. A. Somorjai and P. D. Yang, *J. Am. Chem. Soc.*, 2009, **131**, 5816–5822.
- 4 K. M. Bratlie, H. Lee, K. Komvopoulos, P. D. Yang and G. A. Somorjai, *Nano Lett.*, 2007, **7**, 3097–3101.
- 5 R. M. Rioux, H. Song, M. Grass, S. E. Habas, K. Niesz, J. D. Hoefelmeyer, P. Yang and G. A. Somorjai, *Top. Catal.*, 2006, **39**, 167–174.
- 6 H. Lee, S. E. Habas, S. Kweskin, D. Butcher, G. A. Somorjai and P. D. Yang, *Angew. Chem., Int. Ed.*, 2006, **45**, 7824–7828.
- 7 C. Wang, H. Daimon, T. Onodera, T. Koda and S. H. Sun, *Angew. Chem., Int. Ed.*, 2008, **47**, 3588–3591.
- 8 N. M. Markovic, H. A. Gasteiger and P. N. Ross, *J. Phys. Chem.*, 1995, **99**, 3411–3415.
- 9 N. Tian, Z. Y. Zhou, S. G. Sun, Y. Ding and Z. L. Wang, *Science*, 2007, **316**, 732–735.
- 10 N. Tian, Z. Y. Zhou and S. G. Sun, *J. Phys. Chem. C*, 2008, **112**, 19801–19817.
- 11 Z. M. Peng, H. J. You, J. B. Wu and H. Yang, *Nano Lett.*, 2010, **10**, 1492–1496.
- 12 Z. Y. Zhou, Z. Z. Huang, D. J. Chen, Q. Wang, N. Tian and S. G. Sun, *Angew. Chem., Int. Ed.*, 2010, **49**, 411–414.
- 13 T. S. Ahmadi, Z. L. Wang, T. C. Green, A. Henglein and M. A. El-Sayed, *Science*, 1996, **272**, 1924–1925.
- 14 L. T. Qu, L. M. Dai and E. Osawa, *J. Am. Chem. Soc.*, 2006, **128**, 5523–5532.
- 15 S. Y. Zhao, S. H. Chen, S. Y. Wang, D. G. Li and H. Y. Ma, *Langmuir*, 2002, **18**, 3315–3318.
- 16 J. T. Ren and R. D. Tilley, *Small*, 2007, **3**, 1508–1512.
- 17 J. T. Ren and R. D. Tilley, *J. Am. Chem. Soc.*, 2007, **129**, 3287–3291.
- 18 C. Wang, H. Daimon, Y. Lee, J. Kim and S. H. Sun, *J. Am. Chem. Soc.*, 2007, **129**, 6974–6975.
- 19 S. I. Lim, I. Ojea-Jimenez, M. Varon, E. Casals, J. Arbiol and V. Puentes, *Nano Lett.*, 2010, **10**, 964–973.
- 20 J. Zhang and J. Y. Fang, *J. Am. Chem. Soc.*, 2009, **131**, 18543–18547.
- 21 E. Ramirez, L. Erades, K. Philippot, P. Lecante and B. Chaudret, *Adv. Funct. Mater.*, 2007, **17**, 2219–2228.
- 22 J. B. Wu, J. L. Zhang, Z. M. Peng, S. C. Yang, F. T. Wagner and H. Yang, *J. Am. Chem. Soc.*, 2010, **132**, 4984–4985.